ANTIMICROBIAL AGENTS AND CHEMOTHERAPY, May 2011, p. 2137–2145 Vol. 55, No. 5
0066-4804/11/$12.00 doi:10.1128/AAC.01148-10

Bioactivity and the First Transmission Electron Microscopy Immunogold Studies of Short *De Novo*-Designed Antimicrobial Peptides▽

Marisa Ann Azad,[1]† Heidi Esther Katrina Huttunen-Hennelly,[2]* and Cynthia Ross Friedman[1]

Department of Biological Sciences, Faculty of Science, Thompson Rivers University, 900 McGill Road, Kamloops, British Columbia V2C 5N3, Canada,[1] and Department of Physical Sciences (Chemistry), Faculty of Science, Thompson Rivers University, 900 McGill Road, Kamloops, British Columbia V2C 5N3, Canada[2]

Received 18 August 2010/Returned for modification 22 October 2010/Accepted 28 January 2011

In light of the era of microbial drug resistance, the current study aimed to better understand the relationships between sequence, higher-order structure, and mechanism of action for five designed peptides against multidrug-resistant (MDR) pathogens. All peptides studied were 15 residues long, were polycationic, adopted alpha-helical structures within hydrophobic environments (excluding the D-amino acid-substituted peptide MA-d), and contained N-terminal glycine residues, a novel antimicrobial peptide (AMP) design principle. Increasing hydrophobicity enhanced MICs (≤500 μg/ml to ≤7.4 μg/ml) without significantly increasing hemolytic activity (18% maximum hemolysis at 3,400 μg/ml). To the best of our knowledge, this is the first study to have successfully adapted and used a transmission electron microscopy (TEM) immunogold method to investigate the mechanism of action of short (~15 residues long) AMPs within bacteria. We propose a "floodgate" mechanism to possibly explain membrane deformation and the relative absence of membrane-associated peptides 10 h into incubation.

Infectious diseases account for approximately 13.3 million deaths worldwide each year (34). With the increasing emergence of multidrug-resistant (MDR) microorganisms, the demand for new and more effective antimicrobial agents has never been more urgent. The design of antimicrobial peptides (AMPs) has gained recent attention as a potential solution to the problem of microbial drug resistance, as designed AMPs have been reported to kill MDR organisms rapidly via highly complicated mechanisms of attack (41). It is hypothesized that AMPs may buffer the rate of formation of MDR organisms by employing modes of action that are largely unrecognizable to many pathogenic defense mechanisms (11). Although it is tempting to assume that engineered AMPs will someday revolutionize the drug industry, their design, medical implications, and mechanisms of action are far from being understood completely.

AMPs are virtually ubiquitous in nature (9). Initially, the evolutionary role of AMPs was thought to be limited to innate immunity and their unrivalled ability to interact with and disrupt the membranes of invading pathogens (31). However, in addition to serving as membrane and/or metabolic disruptors of invading viruses, bacteria, fungi, and protozoa, many AMPs also serve as immunomodulatory and signaling agents (20), factors that will undoubtedly shape the future of *de novo*-designed (chemically synthesized) AMPs by adding yet another layer of complexity to the already obscure list of AMP design principles. *De novo*-designed AMPs are generally designed to mimic those found in nature, most of which are polycationic (net charge of +2 to +9), short (6 to 50 residues), and amphipathic (19, 20). In particular, the most abundant AMP class adopts an organized, amphipathic alpha-helix in hydrophobic environments such as the lipid bilayer and an unorganized, flexible structure in hydrophilic environments such as the cytosol (20).

Despite their broad spectrum of activity, some alpha-helical AMPs have been reported to target pathogenic membranes over mammalian membranes, an important characteristic that may be attributed to differences in the relative distribution and/or concentrations of specific membrane components as well as in membrane rigidity and overall hydrophobicity (25, 32). In addition, Gram-positive and Gram-negative bacteria contain negatively charged teichoic acids and the acidic lipopolysaccharide (LPS) layer, respectively. According to the self-promoted uptake theory, alpha-helical AMPs displace cations such as Mg^{2+} and Ca^{2+} on the outer acidic surfaces of bacteria, thereby creating an electrostatic "crack" that facilitates their access to the cytoplasmic membrane (20). Once self-promoted uptake has occurred, alpha-helical AMPs may cause membrane depolarization and subsequent lysis through the formation of highly organized transmembrane pores, dynamic peptide-lipid aggregates, and/or disorganized micelle-like complexes (27, 36). Some AMPs may even spontaneously and randomly "flip" into the cytosol (30) upon interacting with the head groups of specific cytoplasmic lipids and/or by establishing nonspecific nonpolar/polar interactions with cytoplasmic lipids and possibly even proteins. This mechanism appears to be particularly rare among alpha-helical cationic AMPs (30), but it may be an important route of cytosolic entry once a

* Corresponding author. Mailing address: Department of Physical Sciences (Chemistry), Faculty of Science, Thompson Rivers University, 900 McGill Road, Kamloops, BC V2C 5N3, Canada. Phone: (250) 377-6063. Fax: (250) 828-5450. E-mail: hhuttunen@tru.ca.

† Present address: McMaster University, Department of Biochemistry & Biomedical Sciences, M. G. DeGroote Institute for Infectious Disease Research, 1200 Main St. West, Hamilton, ON L8N 3Z5, Canada.

▽ Published ahead of print on 7 February 2011.

TABLE 1. Yields of purified peptides and MALDI-MS characterization of *de novo*-designed peptides[a]

Peptide	Yield (%)	Mass (Da)
Pep-1	82	1,764
MA-d	80	1,764
MAw-1	79	1,895
MAw-2	78	1,967
MAw-3	81	2,038

[a] Calculated and experimental masses agree within 1 Da.

significant amount of membrane disorder has been established by nearby membrane-bound AMPs.

Using molecular dynamic simulations and mathematical modeling, it was recently hypothesized that alpha-helical AMPs may exert a complicated sequence of distinct curvature strains upon the cytoplasmic membrane, eventually leading to the formation of small (~1.5 to 5 nm in diameter), highly disordered, and dynamic toroidal pore aggregates, in contrast to the larger and more established lytic pores predicted by the traditional toroidal model of AMP attack (16, 24, 36). According to the traditional toroidal model, lytic pores are lined with the hydrophilic side chains and bound lipid head groups of AMPs. In the current study, we propose that short (~15 residues) alpha-helical AMPs may rapidly form short-lived toroidal "gaps" composed of small peptide aggregates during the early stages of AMP attack: membrane-bound peptides stress the hydrophobic/electrostatic-rich information of available membrane components, leading to the rapid recruitment of nearby unbound peptides. This "floodgate" mechanism might be limited, in theory, as the number of peptides available for pore formation decreases over time.

MATERIALS AND METHODS

Peptide synthesis and purification. Peptides were synthesized using standard Fmoc solid-phase peptide synthesis (SPPS) techniques on an automated Applied Biosystems model AB1 431A peptide synthesizer. All solvents, coupling reagents, and protected amino acids were purchased from Advanced Chemtech (Louisville, KY). Prior to cleavage reactions, the N terminus of each resin-bound peptide was acetylated by adding 5 ml Ac_2O with 1 ml *N*-methyl-2-pyrrolidone (NMP). The reaction mixture was stirred for 2 h and then vacuum filtered through a medium-pore-size fritted glass funnel. Cleavage of the C-terminal rink resin with 10 ml of 2,2,2-trifluoroacetic acid (TFA) (95:5 TFA:H_2O) for ~10 h yielded a C-terminal amide, and unprotected peptide was recovered via vacuum filtration through a medium-pore-size fritted glass funnel with dichloromethane (DCM) washings (3 times with 10 ml each). The filtrate was rotary evaporated, and 10 ml of cold diethyl ether was added. Three extractions with H_2O (20 ml each) were performed on each peptide. Peptides were purified using a Waters PrepLC 4000 system with a C_{18} reverse-phase column (250 × 21.20 mm, 300-Å pore size, 10-μm particle size). Prior to injection (1 ml), samples were filtered through a 0.45-μm nylon syringe filter (Phenomenex). Samples were run at a flow rate of 10 ml min^{-1}, using helium-sparged filtered H_2O (0.1% TFA) and high-performance liquid chromatography (HPLC)-grade acetonitrile (0.05% TFA) gradients. The UV detector was set at 220 nm. Purified samples (>95% pure) were then rotary evaporated, and 1 ml from each sample was vacuum centrifuged overnight (45°C) on a Vacufuge 5301 centrifugal vacuum concentrator. Peptide masses were confirmed by running samples on a Perseptive Biosystems Voyager Elite matrix-assisted laser desorption ionization–time of flight mass spectrometer (MALDI-TOF MS) with delayed extraction, using 50 μM cinnamic acid in 1:1 H_2O:MeCN (0.1% TFA) as the matrix (Table 1), and peptides were determined to be >95% pure by analytical reverse-phase HPLC. A Bio-Rad protein concentration kit using a Lowry (5) colorimetric assay was used to determine peptide concentrations. Absorbance was measured at 750 nm using a Cary UV-visible spectrophotometer.

CD spectroscopy and ^{1}H nuclear magnetic resonance (NMR) spectroscopy. A Jasco J-810 spectrometer was used to record circular dichroism (CD) spectra at the University of British Columbia (UBC) Laboratory of Molecular Biophysics. Samples were analyzed in triplicate under hydrophilic (50 mM phosphate buffer) and hydrophobic (50 mM phosphate buffer with 50% trifluoroethanol [TFE]) conditions with final peptide concentrations of ~50 μM. Three scans were averaged and subtracted from a background scan to produce final spectra. Final spectra were normalized to the mean residue ellipticity (θ) as defined by the following equation: $\theta = \theta_{obs}/10lcn$, where θ_{obs} is the observed ellipticity (mdeg), l is the path length (cm), c is the peptide concentration (mol $liter^{-1}$), and n is the number of residues in the peptide. The average error was ±5%. Individual samples were run three different times to ensure reproducibility.

For NMR, a 500-MHz Bruker Avance AMIII 500 spectrometer and a TXI probe with H_2O suppression were used. Samples were dissolved in 9:1 sodium phosphate buffer (50 mM; pH 7.0)-D_2O with a final peptide concentration of ~1.5 mM.

Antimicrobial activity. Test microorganisms (Gram-positive *Staphylococcus aureus* and methicillin-resistant *Staphylococcus aureus* [MRSA], Gram-negative *Escherichia coli*, *Pseudomonas aeruginosa*, and *Salmonella enterica* serovar Enteritidis, and eukaryotic *Candida albicans*) were grown to mid-logarithmic phase in Mueller-Hinton broth on an orbital shaker (37.5°C, 175 rpm) and diluted to a 0.5 McFarland standard with a final volume of 1 ml. Decreasing concentrations of peptide (1,000 μg/ml to 0.01 μg/ml) were incubated and shaken with microorganisms (24 h, 37.5°C). Absorbances were read at 400 nm in duplicate, using an LKB Novaspec II spectrophotometer (Pharmacia). The MIC was defined as the concentration resulting in ≥85% killing of the initial inoculums. All samples were prepared in triplicate and run three separate times to ensure reproducibility.

Hemolytic activity. Minimum inhibitory hemolysis was defined as ≥85% hemolysis of erythrocytes. Erythrocytes were washed (and subsequently centrifuged) five times with 100 mM sodium phosphate buffer (pH 7.4). Cells were diluted 10-fold to produce a stock solution containing ~5×10^8 cells/ml. A 1% Triton X-100 solution was used as a positive control, whereas 100 mM sodium phosphate buffer (pH 7.4) was used a negative control and blank. Increasing concentrations of peptides were incubated with erythrocytes (1 h, 37.5°C). Samples were gently inverted 10 times 30 min into incubation. Samples were centrifuged for 5 min at 14,000 rpm, and the amount of hemoglobin in each supernatant was measured at 541 nm. All samples were prepared in triplicate and run three separate times to ensure reproducibility. Percent hemolysis was defined as follows: [(sample absorbance − phosphate buffer absorbance)/Triton X-100 absorbance] × 100.

TEM immunogold method. *Staphylococcus aureus* was grown to mid-logarithmic phase in Mueller-Hinton broth. Peptide (1,000 μg/ml)-containing cultures were incubated with shaking (10 h, 37.5°C). Samples were then centrifuged (5,000 rpm, 5 min), and the supernatant was discarded. A 1-ml portion of Karnovsky's fixative solution (4% paraformaldehyde, 5% glutaraldehyde, 2.5 mM phosphate buffer [pH 6.8]) was added, and samples were mixed gently for 5 h on a rotator. Samples were then centrifuged (5,000 rpm, 5 min), and excess fixative solution was discarded. A 1-ml aliquot of 0.1% glycine solution was added, and samples were inverted gently for 1 h. Samples were centrifuged again (5,000 rpm, 5 min), and the supernatant was discarded and suspended in 0.5 ml of liquid low-melting-point agarose (cooled to 45°C). Once the samples solidified, the gels were removed, dehydrated in increasing concentrations of ethanol (30%, 50%, 70%, and 90% ethanol for 20 min each and, finally, 100% anhydrous ethanol [thrice] for 20 min each time), placed in the following solutions, and inverted gently: 1:1 solution of LR White resin and 100% anhydrous ethanol (1 h), 3:1 solution of LR White resin and 100% anhydrous ethanol (1 h), and 100% LR White resin (twice for 3 h each). Samples were then transferred to Beem tubes (1 sample/tube), and tubes were filled with LR White-accelerator solution (2 drops of accelerator per 10 ml of LR White). Samples were left overnight to solidify. The primary antibody was prepared by GenScript Corp. (Piscataway, NJ) via immunization of rabbits with peptide. Immunolabeling and staining were performed according to the methods of Ross Friedman et al. (33). A Leica EM IGL automated immunogold labeling system (Leica, Richmond Hill, Canada) at the UBC was used for immunolabeling. Grids containing ~50-nm sections (~15 median sections were made for the treatment and each control; only 1 median section was produced per cell) were treated with a 1% bovine serum albumin–0.1 M phosphate buffer solution (pH 7.4) for 30 min and then incubated with 1:25-diluted anti-MAw-1 for 1 h. Sections were then rinsed in 1% bovine serum albumin–0.1 M phosphate buffer (three times for 10 min each) and incubated with 1:100-diluted 10-nm colloidal gold anti-rabbit (Pelco International) for 1 h. Sections were visualized with 2% aqueous uranyl acetate (20 min). Sato's lead was used as the counterstain for enhanced resolution. The following controls

TABLE 2. Overall characteristics of the five *de novo*-designed peptides[a]

Peptide	Sequence[b]	Secondary structure		Boman index (kcal/mol)	Total proportion (%)[c]			
		Aqueous environment	TFE environment		HB	HP	Gly	Trp
Pep-1	CH_3CO-GKKLLKKLKKLLKKG-NH_2	α-Helix	α-Helix	1.19	33	53	13	0
MA-d	CH_3CO-GKK<u>LL</u>KK<u>L</u>KK<u>LL</u>KKG-NH_2	Extended	Extended	1.10	33	53	13	0
MAw-1	CH_3CO-GKKLLKKLKKLLKK**W**-NH_2	α-Helix	α-Helix	1.10	40	53	6	6
MAw-2	CH_3CO-GKKLLKKLKKL**W**KK**W**-NH_2	Partial α-helix	α-Helix	1.27	40	53	6	13
MAw-3	CH_3CO-GKKLLKK**W**KKL**W**KK**W**-NH_2	Partial α-helix	α-Helix	1.44	40	53	6	20

[a] CD and one-dimensional ^{1}H NMR were used to determine peptide secondary structure. Each peptide was analyzed in aqueous (phosphate buffer) and hydrophobic (phosphate buffer with TFE) environments to predict its structure within the cytoplasmic membrane and cytosol of pathogens, respectively.
[b] Underlined amino acids are D-amino acids. Amino acids in bold are tryptophan substitutions.
[c] HB, HP, Gly, and Trp, total percentages of hydrophobic, hydrophilic, glycine, and tryptophan residues, respectively.

were prepared: (i) no peptide-no primary antibody-secondary antibody, (ii) no peptide-primary antibody-secondary antibody, and (iii) peptide-no primary antibody-secondary antibody. Images were taken by transmission electron microscopy (TEM) using a Hitachi model H-7600 electron microscope (80 kV) (Hitachi, Tokyo, Japan).

RESULTS

Peptide design and synthesis. Alignment studies have shown that ≥70% of naturally occurring AMP N-terminal amino acids are glycine residues (42). Despite this fact, the incorporation of N-terminal glycine residues has yet to be acknowledged as an important AMP design principle. Helical propensity, the thermodynamic "ease" with which an amino acid (and resulting peptide) will spontaneously form an alpha-helix, has been reported to play an important and complicated role in AMP bioactivity (8). Specifically, every amino acid has an associated helical propensity value, ranging from the highest propensity value for alanine to the lowest propensity value for glycine, excluding proline (28). Glycine residues therefore serve as alpha-helix breakers in that they disrupt alpha-helix formation (17). Thus, by incorporating glycine residues at the N terminus of each peptide, it was hypothesized that glycine would "cap" the peptides and prevent them from losing their helicity or "unraveling" within pathogenic cells (Table 2). To the best of our knowledge, this design principle has never before been investigated as a means to enhance the bioactivity of alpha-helical AMPs. The overall helix dipole of each AMP was protected via the incorporation of acetylated and amidated N and C termini, respectively (23).

As a general AMP design principle, the number of hydrophobic residues is proportional to hemolytic and antimicrobial activities and the number of positively charged residues is proportional to antimicrobial activity and inversely proportional to hemolytic activity (2, 26). Cationic AMPs are composed of ≥50% hydrophobic residues (30). Positively charged residues may buffer the hemolytic effect of hydrophobic residues, and in order to minimize cytotoxicity, the hydrophilic/hydrophobic residue ratio of the *de novo* AMPs was elevated substantially, such that each peptide had a charge of +8 and a total hydrophobicity count of ~37%.

To determine how important helicity was to AMP bioactivity, helicity was disrupted through the incorporation of symmetrically distributed D-amino acids (MA-d). The Boman index estimates the potential for a protein to bind to other proteins (4). In other words, a high Boman index value indicates that an AMP will be multifunctional or play a variety of different roles within the cell due to its ability to interact with a wide range of proteins. All of the AMPs used in this study were designed to have intermediate Boman index values according to the online Antimicrobial Peptide Database (http://aps.unmc.edu/AP/main.php). Other design principles taken into account included the symmetrical distribution of amino acids and the presence of lysine repeats. Lysine repeats (positioned every fourth or fifth position) are common among naturally occurring alpha-helical AMPs such as the lycotoxins and magainins, and they are believed to be important for establishing peptide-membrane interactions (40). Following their design, peptides were synthesized using standard Fmoc SPPS techniques on an automated peptide synthesizer as outlined by the manufacturer (yields were ~80%) (see Materials and Methods).

Structural characterization. CD was used to evaluate peptide secondary structure. Strongly alpha-helical peptides produce large negative bands at ~222 nm and ~208 nm and a large positive band at ~193 nm (12, 18). Each peptide was analyzed in hydrophilic (phosphate buffer) and hydrophobic (phosphate buffer with TFE) environments to predict its structure within the cytoplasmic membrane and cytosol of pathogens, respectively (Fig. 1). Pep-1 contained two glycine caps as well as the largest number of helix-stabilizing amino acids such as leucine, and it was therefore predicted that this peptide would exhibit the highest degree of helicity. It was also predicted that increasing the number of tryptophan substitutions for leucine and/or glycine residues would decrease helicity. Figure 1 supports these predictions. MAw-1 showed the highest degree of helicity among the three tryptophan-substituted peptides, followed by MAw-2 and then MAw-3. With the exception of the extended peptide MA-d, all of the peptides adopted a more helical structure in TFE, as demonstrated by larger signals. The weak signal produced by MA-d is characteristic of a random coil (12).

One-dimensional ^{1}H NMR is a simple diagnostic tool that may be used to elucidate peptide structure and flexibility. Slowly exchanging amide protons typically confer distinct signals between 7 and 11 ppm (7, 29, 39). In Fig. 2a, the overlapping signals of MA-d clearly show that it is a highly flexible molecule with a poorly defined secondary structure that is not alpha-helical. The poorly defined amide region of MA-d supports a random coil secondary structure, which is consistent with its undefined CD spectrum. As predicted, MAw-1 exhib-

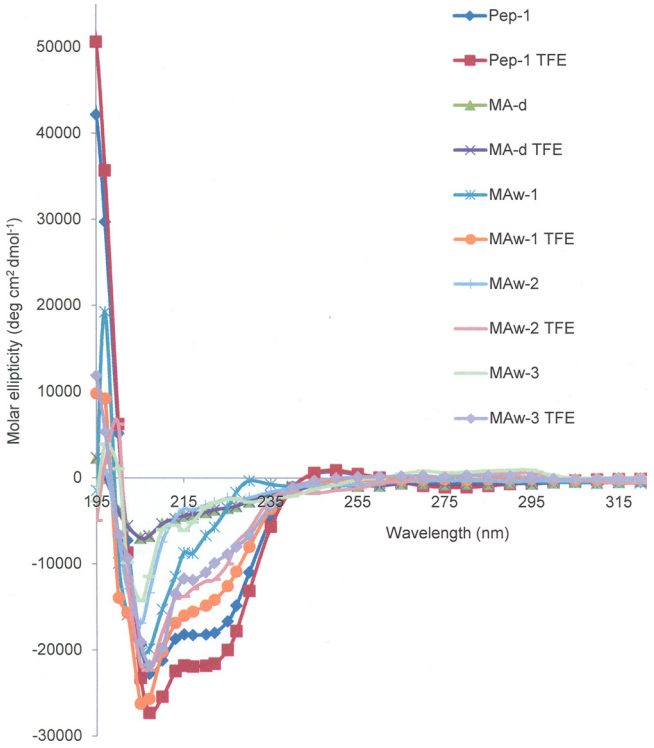

FIG. 1. Overlay of individual peptide CD spectra at ~50 μM in aqueous (phosphate buffer) and hydrophobic (phosphate buffer with TFE) environments (pH 7; 20°C). All of the peptides are alpha-helical, with the exception of MA-d, which has a CD curve characteristic of a random coil. As the number of tryptophan residues in the peptide sequences was increased, a decrease in alpha-helicity was observed. TFE was found to increase the helicity of all peptides except for MA-d.

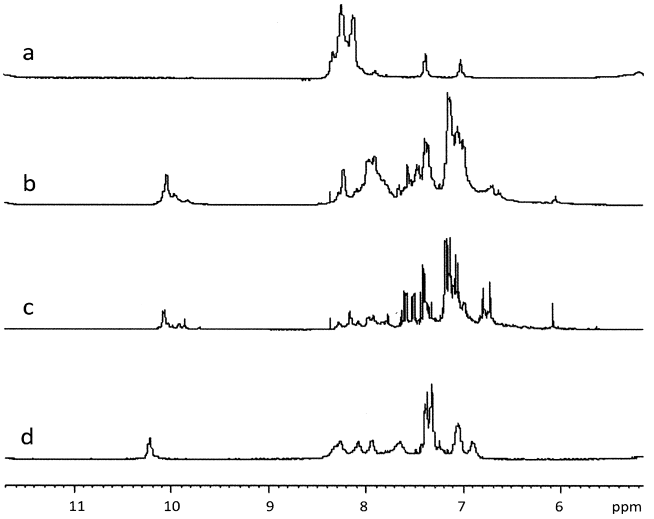

FIG. 2. Expansions of amide regions of 500-MHz ^{1}H NMR spectra for MA-d (a), MAw-3 (b), MAw-2 (c), and MAw-1 (d) at ~1.5 mM in 10% D_2O–45 mM phosphate buffer (pH 7.0) at 20°C. The overlapping signals of MA-d (a) show that it is a highly flexible molecule with a poorly defined secondary structure that is not alpha-helical. MAw-1 exhibited a greater separation of signals within the amide region (indicative of an alpha-helical structure) than did MA-d, due largely to the absence of helix-disrupting D-amino acids. Among the three tryptophan-containing peptides, MAw-1 (d) demonstrated the least conformational flexibility, as supported by the presence of only one tryptophan NH signal, at ~10.2 ppm. MAw-2 and MAw-3 (c and d, respectively) produced more tryptophan NH signals (~10 ppm) than expected and therefore likely have more than one conformation in solution.

ited a greater separation of signals within the amide region (which is indicative of an alpha-helical structure) than MA-d, due largely to the absence of helix-disrupting D-amino acids (Fig. 2d). Among the three tryptophan-containing peptides, MAw-1 demonstrated the least conformational flexibility (it was quite alpha-helical even in an aqueous environment, according to its CD spectrum), as supported by the presence of only one tryptophan NH signal, at ~10.2 ppm. Because MAw-2 and MAw-3 produced more tryptophan NH signals (~10 ppm) than expected (Fig. 2c and b, respectively), they likely populated more than one conformation in solution. This is in agreement with the smaller amount of alpha-helicity observed in an aqueous environment in their CD spectra. It is likely that the secondary structures of MAw-2 and MAw-3 alternate between an alpha-helix and a random coil conformation.

Antimicrobial activity. Using a turbidity assay, it was determined that the peptides (with the exception of MA-d) were active against a wide range of different microorganisms (Table 3). Pep-1 was most active against Gram-negative *S. enterica* serovar Enteritidis (≤500 μg/ml) and Gram-positive *P. aeruginosa* (≤500 μg/ml). To study the importance of helicity in the bioactivity of these AMPs, MA-d was created. As predicted, disrupting the strongly helical nature of Pep-1 resulted in the complete suppression of its antimicrobial activity. The fact that MA-d did not kill any microorganisms suggests that the mechanism of action of Pep-1 (and possibly that of the three tryptophan-substituted AMPs) relies on a high degree of helicity during some stage of attack. Increasing the number of tryptophan residues greatly enhanced the antimicrobial activity of Pep-1. MAw-1 was effective against every test microorganism except for *E. coli*, with MICs of ≤100 μg/ml. MAw-2 and MAw-3 were both effective against *E. coli* (MICs of ≤530 μg/ml and ≤74 μg/ml, respectively) as well as every other test microorganism, except for MRSA. Both MAw-2 and Maw-3 were active against *C. albicans*, with MICs in the μg/ml range.

Figure 3 shows an interesting and unpredicted phenomenon that occurred with MRSA–MAw-1 and *P. aeruginosa*–MAw-1 samples: MAw-1 lysed more *P. aeruginosa* cells at a lower concentration (100 μg/ml) than at a higher concentration (1,000 μg/ml). This phenomenon was also observed with the *C. albicans*–MAw-2 sample as well as with all MAw-3 samples except the MRSA–MAw-3 sample. In these cases, higher concentrations of peptide may have triggered the activation of one or more microbial defense mechanisms.

Hemolytic activity. Tryptophan is particularly prevalent among naturally occurring AMPs, and it has been shown to increase both the antimicrobial and hemolytic activities of AMPs due to its ability to interact strongly with hydrophobic membrane components (35, 43). It was therefore predicted that MAw-3 would exhibit the highest percentage of hemolysis, followed by MAw-2, MAw-1, and Pep-1/MA-d. Pep-1 and its D-amino acid-substituted derivative MA-d were predicted to display similar hemolysis curves. D-Amino acids have been

TABLE 3. Comparison of MICs obtained by a turbidity assay in which increasing concentrations of peptides were incubated with each microorganism for 24 h[a]

Peptide	MIC (μg/ml) (mean ± SD)					
	E. coli	*S. enterica* serovar Enteritidis	*P. aeruginosa*	*S. aureus*	MRSA	*C. albicans*
Pep-1	≫500 ± 10	≤500 ± 10	≤500 ± 10	>1,000	≫500 ± 10	>1,000
MA-d	>1,000	>1,000	>1,000	>1,000	>1,000	>1,000
MAw-1	>1,000	≤100 ± 10	≤100 ± 20	≤100 ± 20	≤100 ± 10	≤100 ± 20
MAw-2	≤530 ± 20	≤530 ± 20	≤530 ± 20	≤530 ± 20	>1,000	≤5.8 ± 0.3
MAw-3	≤74 ± 1	≤74 ± 1	≤74 ± 2	≤74 ± 3	>1,000	≤7.4 ± 0.1

[a] The MIC was defined as the concentration resulting in ≥85% lysis compared to that in control cultures. Pep-1 showed minimal activity against *E. coli* and MRSA.

reported to lower the hemolytic activity of AMPs (8), and it was found that MA-d was only slightly more hemolytic than Pep-1 (1.0% versus 0.3% hemolysis) (Fig. 4). This could have resulted from the increased flexibility in structure for MA-d, allowing for a higher probability of the establishment of nonspecific electrostatic interactions and subsequent translocation through the outer leaflet of erythrocytes. The hemolytic activity was highest with MAw-3 (18%) and (unexpectedly) with MAw-1 (17%), although in both cases hemolysis was minimal. Recall that increases in hydrophobicity and helicity (8) have been shown to increase the hemolytic activity of AMPs (29, 35, 43). MAw-1 was the most helical of the three tryptophan-substituted AMPs, as demonstrated by its NMR and CD (TFE) spectra. However, helicity cannot be wholly responsible for the enhanced hemolytic activity of MAw-1, as the most helical peptide (Pep-1) produced the lowest percentage of hemolysis.

All active peptides exhibited <5% hemolysis at their MICs, and thus their pharmaceutical potential is promising (no hemolytic index could be calculated because the active peptides did not reach 100% hemolysis at the concentrations tested).

TEM. To the best of our knowledge, TEM immunogold analysis has never been used to localize short (≤15 amino acids in length) alpha-helical AMPs within bacterial cells. Figure 5 contains representative TEM images of *S. aureus* after 10 h of incubation with MAw-1. Upon initial investigation, it was immediately noted that the cytoplasmic membrane, peptidoglycan layer, and outer acidic surfaces of peptide-treated cells (Fig. 5c to e) were deformed in comparison to the round appearance of control cells (Fig. 5a and b). Peptide-treated cells no longer appeared to be undergoing replication, as indicated by the disappearance of the binary fission division line. Interestingly, there were few MAw-1 peptides associated with the bacterial membrane. Despite this fact, Fig. 5c to e show widespread membrane deformation. Figure 5e shows the few peptides that were closely associated with the cytoplasmic membrane, designated by black boxes. Membrane-associated peptides in Fig. 5e seem to be positioned next to small membrane folds (black arrows) that may represent an aggregation of previously established (<10 h of incubation) toroid-like pores. From Fig. 5, it would appear that MAw-1 does not interact preferentially with DNA.

DISCUSSION

In this study, we investigated the relationships between sequence, secondary structure, and mechanism of action for *de novo*-designed alpha-helical polycationic peptides. Taken together, the NMR and CD data determined that Pep-1 was highly alpha-helical in both aqueous and hydrophobic environments, whereas the three tryptophan derivatives were alpha-helical in a hydrophobic environment only, and that MA-d was a random coil regardless of the chemical environment (Table 2; Fig. 1). Incremental tryptophan substitutions decreased the degree of helicity of the *de novo*-designed peptides. This conclusion is reasonable, as tryptophan residues have lower helical propensities than leucine residues (0.28 kcal/mol less than that of leucine) (28). The extended structure of MA-d may be insufficient to establish strong electrostatic and hydrophobic interactions with components of microbial membranes. Losing the distinct hydrophobic and hydrophilic faces of these peptides may therefore be critical to their bioactivity in terms of oligomerization and other membrane-disrupting activities.

Many of the design principles used during this study have never before been combined. The bioactivity data are suggestive of the importance of N-terminal glycine caps in concert with tryptophan substitution for the design of potent, nonhemolytic alpha-helical cationic AMPs (Table 3; Fig. 4). The inactivity of the AMPs against *E. coli*, *S. aureus*, MRSA, and *C. albicans* may be attributed to the presence of proteolytic enzymes (1, 22, 38), a mode of pathogenic resistance that has yet to be elucidated fully in relation to AMPs. Moreover, multi-

FIG. 3. Turbidity assay results with decreasing concentrations of MAw-1 (from left to right, 1,000 μg/ml to 0.01 μg/ml) against *P. aeruginosa*. Samples were taken in triplicate. Note that the highest concentration of peptide did not produce the greatest amount of lysis. This effect may have been caused by the activation of one or more defense mechanisms against the peptide. In addition, it is also possible that MAw-1 interacts optimally with itself to induce killing at 100 μg/ml.

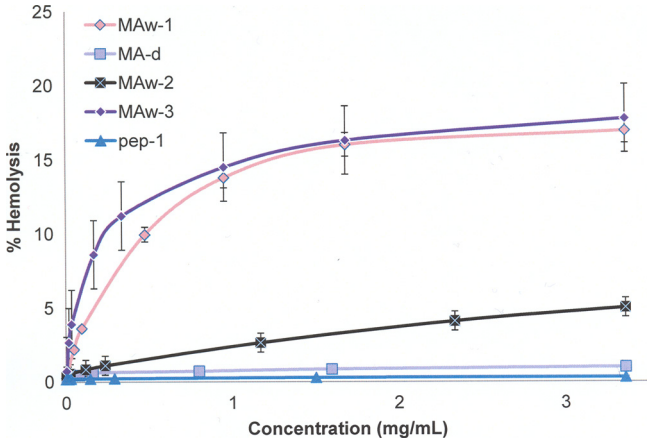

FIG. 4. Hemolytic activities of *de novo* peptides after 1 h of incubation with erythrocytes. Hemoglobin leakage was measured by reading absorbances at 541 nm. All peptides exhibited minimal hemolysis (18% maximum hemolysis at 3.4 mg/ml [3,400 μg/ml]), and as a result, minimal hemolytic concentrations were unable to be calculated. Minimal hemolytic concentrations were defined as ≥85% hemolysis.

drug efflux pumps may also have contributed to resistance against the *de novo* AMPs (10). Furthermore, some AMPs have been reported to trigger pathways that result in an increase in the stability of the outer acidic surfaces and/or cytoplasmic membrane. For example, *P. aeruginosa* and *S. enterica* serovar Enteritidis are particularly difficult to treat with antibiotics due to their use of the PhoP/PhoQ two-component regulatory system that is triggered in response to a decrease in the LPS-associated Mg^{2+} concentration (21). This microbial defense mechanism (or one very similar to it) may have resulted in the phenomenon shown in Fig. 3. This phenomenon may also be explained by the AMP demonstrating concentration-dependent oligomerization: perhaps the AMP interacted optimally with itself to lyse pathogens at lower concentrations. Another possibility might be that the peptide was primarily bacteriostatic at the lower concentration.

Regarding the higher-than-expected hemolytic activity of MAw-1 (Fig. 4), it is possible that this peptide strikes a balance between the conflicting factors of helicity and hydrophobicity. Recall that MAw-1 exhibited a maximum hemolysis value of

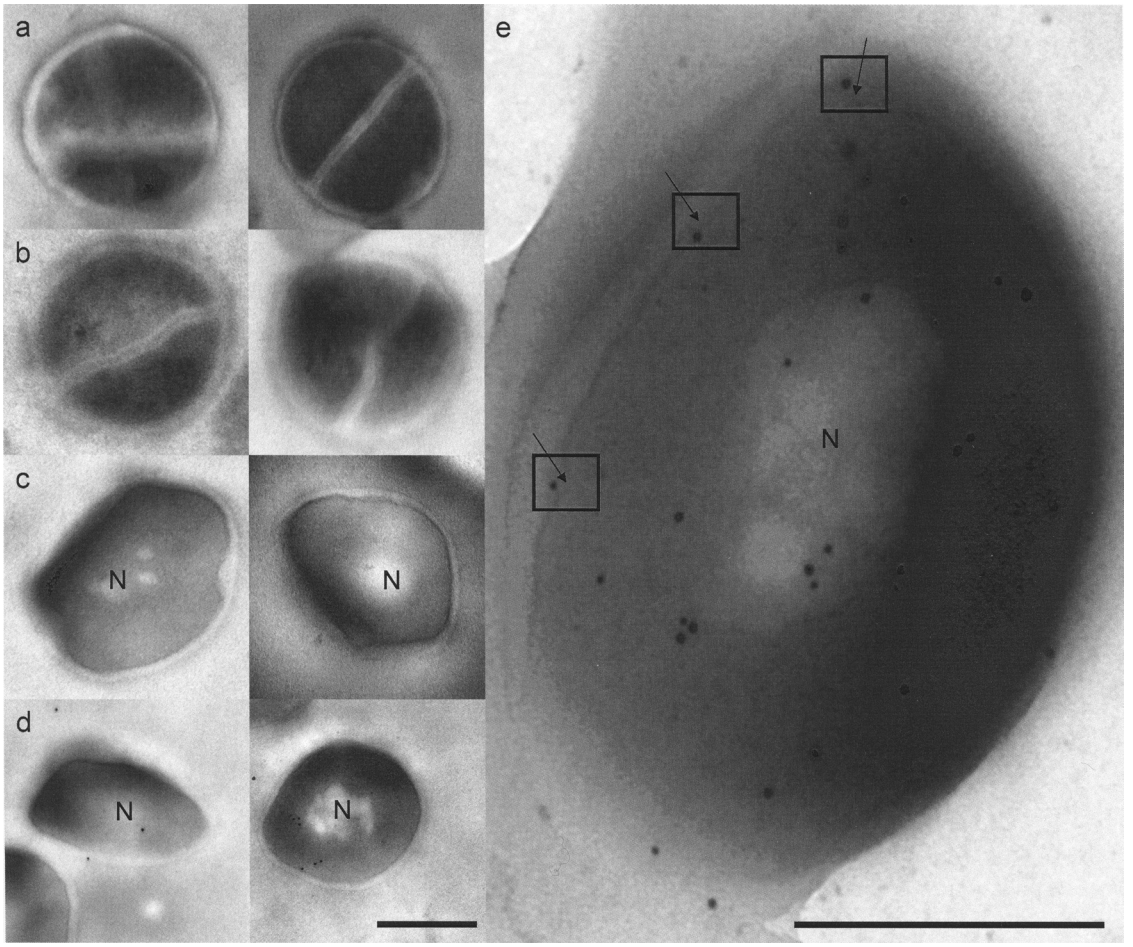

FIG. 5. Representative TEM immunogold images of *S. aureus* cells incubated with MAw-1 (10 h). (a, b, and c) Control samples (no peptide-no primary antibody-secondary antibody, no peptide-primary antibody-secondary antibody, and peptide-no primary antibody-secondary antibody, respectively). (d and e) Experimental samples containing peptide and primary and secondary antibodies. Peptides did not appear to interact preferentially with DNA, as designated by "N" (nucleoid). Bacterial replication seemed to have arrested. Widespread membrane disruption occurred despite the paucity of peptides associated with the membrane. The black arrows in panel e indicate membrane disruptions that may be attributed to adjacent peptides (black boxes). Bars, 0.5 μm.

17% and that MAw-2 and MAw-3 produced maximum hemolysis values of 5.0% and 18%, respectively (Fig. 4). The strong degree of helicity in MAw-1 (as outlined by the CD and NMR data) may allow for better penetration of the C-terminal tryptophan residue and therefore a more efficient mechanism of attack against the zwitterionic membrane of erythrocytes. To our knowledge, the possibility that some AMPs could use helicity to enhance the membrane permeabilization activity of C-terminal tryptophan residues has never before been explored.

Because these peptides demonstrated minimal hemolysis as well as potent antimicrobial activity (excluding MA-d), they hold great promise as pharmaceutical agents (particularly MAw-1, MAw-2, and MAw-3). All three of these peptides exhibited a broad spectrum of activity against Gram-negative and Gram-positive cells and eukaryotic yeast cells. The fact that MAw-2 and MAw-3 were active against *C. albicans*, with MICs in the μg/ml range, is very exciting indeed.

The MAw-1 peptide is too short (~2.25 nm) to span the cytoplasmic membrane, which is ~8 to 9 nm in diameter (30). Because of this fact, it is unlikely that MAw-1 lyses cells via transmembrane pore formation. Rather, MAw-1 may follow a toroidal model or some derivative thereof (note that the carpet model is merely an extreme case of the toroidal model, and it is also excluded from this discussion due to the observation that few peptides were found associated with the bacterial cytoplasmic membrane). Figure 5c to e demonstrated that *S. aureus* suffered extensive membrane deformation despite there being few membrane-associated peptides. Thus, the question remains as to why no cell contained concrete evidence of interacting peptides (or pore formation) within the cytoplasmic membrane. The discussion outlined below aims to answer this question by proposing the following mechanism of attack for MAw-1 against *S. aureus* (Fig. 6): (i) MAw-1 forms small (~3 peptides), dynamic toroidal pores within the cytoplasmic membrane which stress the hydrophobic/electrostatic-rich information of available membrane components (<10 h of incubation); (ii) the subsequent increase in membrane disorder and hydrophobic/electrostatic-rich information leads to the rapid kinetic and thermodynamic recruitment of nearby unbound peptides (<10 h of incubation); (iii) this "floodgate" effect is limited as the number of peptides available for pore formation decreases over time, which in turn favors pore dissipation and the rapid release of previously membrane-bound peptides into the cytosol (<10 h of incubation); (iv) following the dissipation of most pores, only toroidal "gaps" or remnants of toroidal pore activity remain (10 h of incubation, the time at which TEM images were captured); (v) toroidal gaps become exaggerated over time due to the continuous leakage of cellular and extracellular contents (>10 h of incubation); and (vi) cytoplasmic membranes collapse (~24 h of incubation).

First, although AMPs have been reported to randomly "flip" into the cytosol, these events are believed to be quite rare (30). Even if the flip-flop model of AMP entry is more common than initially proposed, it is unlikely that such an event would be wholly responsible for full cellular lysis at ~24 h of incubation, as the disruptions in membrane potential following each peptide flip should rapidly dissipate once the peptide has reached the cytosol. It is also unlikely that MAw-1 "leaks" into membranes as many hydrophobic AMPs do, as MAw-1 has a distinct hydrophilic face that should prevent this process from dominating. Excluding these two possibilities for MAw-1 entry, we must once again address the toroidal model.

In general, toroidal pores are short-lived and highly dynamic (24, 36). Using membrane simulations, it was recently reported that just 3 melittin molecules (an alpha-helical cationic AMP of 26 residues in length) may aggregate to form disorganized, small (~1.5 nm in diameter), toroidal pores in artificial membranes within ~10 to 100 ns (36). Given such a high rate of formation, it is possible that the collapse of these pores could be just as rapid. Because so few peptides were found associated with *S. aureus* membranes (Fig. 5c to e), it is unlikely that large aggregates of MAw-1 were involved in the formation of toroidal pores as outlined by the traditional toroidal model. It has also been proposed that pore dissipation may lead to the translocation and influx of previously pore-associated peptides into the cytosol (13, 24).

The exact kinetic and thermodynamic mechanisms for the establishment and dissipation of toroidal pores have yet to be elucidated fully; however, it is known that membrane-bound peptides exist in equilibrium with unbound peptides and that the membrane potential (E_M, ~125 mV) and the presence of negatively charged, hydrophobic, and possibly even hydrophilic membrane components could all serve as powerful driving forces for the binding of peptides to the membrane (13, 24). Membrane-bound peptides may induce a positive curvature upon the membrane (pushing the lipid head groups apart) and then a negative curvature to allow for toroidal pore formation (6, 24, 37). Membrane curvature could very well lead to an increase in the exposure of hydrophobic tails and/or electrostatic head groups of nearby phospholipids, thereby allowing for an even greater energetic potential for the establishment of peptide-membrane interactions.

We propose that this increase in the amount of hydrophobic/electrostatic-rich information within the membrane could lead to the rapid recruitment of nearby unbound peptides (<10 h into incubation). However, this "floodgate" effect, in theory, will become less prominent over time as the number of peptides available for pore formation decreases. Once a threshold concentration of membrane-bound peptides is reached, an increase in membrane disorder could lead to an increase in the number of peptide flip-flop events, a process that may play an important role during the last stages of AMP attack. Furthermore, during pore dissipation, membrane-bound peptides could migrate to the cytosolic leaflet before being released into the cytosol due to shifts in thermodynamic and kinetic stability (15, 16, 36), and possibly even due to changes in environmental conditions (e.g., higher concentrations of salt within the cytosol could disrupt the electrostatic disruptions of peptides bound to the inner lining of toroidal pores).

Given the above discussion, it is possible that our TEM images captured toroidal pore remnants or "gaps" 10 h into incubation. That is, we likely just missed the rapid influx of peptides as outlined by the proposed floodgate mechanism, a process that appears to be in accordance with Huang's modeling of AMP cooperativity and the free energies associated with pore formation (15, 16). In addition, it is also possible that toroidal pores are relatively rare occurrences within the microbial membrane in this instance. It is important that although many TEM images were taken, there are millions of cells, each

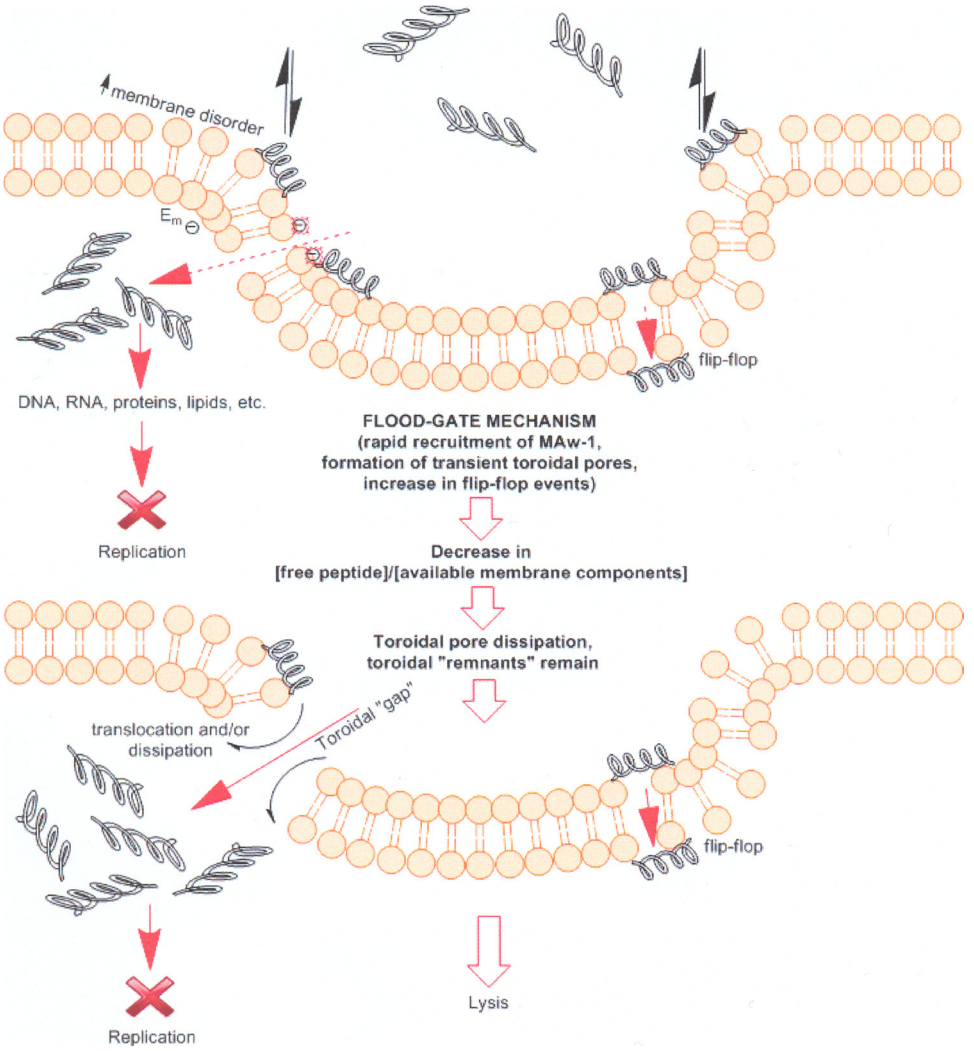

FIG. 6. Proposed floodgate mechanism of attack for MAw-1 against *S. aureus*. Membrane-bound peptides exist in equilibrium with unbound peptides. The membrane potential (E_M) and the presence of negatively charged hydrophobic and possibly even hydrophilic membrane components all serve as powerful driving forces for the binding of peptides to the membrane. Membrane-bound peptides induce a negative curvature upon the membrane that allows for toroidal pore formation. This leads to an increase in the amount of hydrophobic/electrostatic-rich information available to nearby peptides, thereby allowing for an even greater energetic potential for the establishment of peptide-membrane interactions. Over time, the concentration of peptides available for pore formation decreases, thus favoring pore dissipation and the translocation of previously bound peptides. Following toroidal pore dissipation, pore remnants or "gaps" remain, eventually leading to cellular lysis.

with a surface area of ~6 μm (41), and that toroidal pores may be as small as ~1.5 nm in diameter (3, 36). This "needle-in-a-haystack" problem may therefore have partially accounted for the lack of membrane-associated peptides.

Once inside the cell, MAw-1 could interfere with a variety of different cellular materials, including DNA, RNA, proteins, lipids, and even smaller components such as divalent cations. Because very few peptides were visualized within the nucleoid region, it is unlikely that they interact preferentially with DNA; however, without further studies, DNA–MAw-1 interactions cannot be ruled out fully. The AMP-induced arrest in replication may have resulted from MAw-1 specifically interfering with one or more of the many molecules involved with binary fission (e.g., Fts proteins) and/or peptidoglycan synthesis (14). Note that MAw-1 may therefore have a two-pronged mode of attack that targets both cellular division and the integrity of the cytoplasmic membrane. It is also possible that replication arrested as a general defense mechanism against the peptide.

In conclusion, the relationships between sequence, structure, and antimicrobial and hemolytic properties of the designed alpha-helical polycationic AMPs Pep-1, MA-d, MAw-1, MAw-2, and MAw-3 were investigated. Using TEM immunogold analysis, a novel mechanism of attack for short, polycationic alpha-helical AMPs was put forth. This model is based upon the formation of transient (small) toroidal pores, as well as a "floodgate" and a phenomenon involving the free peptide/available membrane component ratio that in theory would limit the number and size of formed lytic pores.

Pep-1, MAw-1, MAw-2, and MAw-3 exhibited potent antimicrobial activity as well as minimal hemolytic activity against a broad spectrum of serious pathogens, and they could very well someday serve as effective antibiotics. These peptides

were carefully created using design principles that have never been used. In particular, this study suggests that N-terminal glycine caps should seriously be considered part of an alpha-helical AMP design principle. If these peptides are to someday become effective antibiotics, then future work should focus upon the determination of the immunomodulatory effects of these peptides, as well as other cytotoxic effects. A TEM immunogold time series would provide invaluable insight into the mechanism of action of these fascinating AMPs. Other studies might focus upon determining whether specific bacterial targets exist for these AMPs.

ACKNOWLEDGMENTS

We thank the Natural Sciences and Engineering Research Council of Canada (NSERC) and the Thompson Rivers University (TRU) Comprehensive University Enhancement Fund (CUEF) for their generous financial support.

We thank G. Martens and B. Ross of the University of British Columbia (UBC) BioImaging Facility for their expertise in transmission electron microscopy. Additional acknowledgments are given to C. Fardy for providing test microorganisms and assistance with blood donations, to T. Hammer for servicing instrumentation, and to F. Rossell and G. Mauk for the use of their Varian Cary Eclipse spectrophotometer at UBC.

REFERENCES

1. **Bernardo, S. M., Z. Khalique, J. Kot, J. K. Jones, and S. A. Lee.** 2008. Candida albicans VPS1 contributes to protease secretion, filamentation, and biofilm formation. Fungal Genet. Biol. **45:**861–877.
2. **Bessalle, R., et al.** 1993. Structure-function studies of amphiphilic antibacterial peptides. J. Med. Chem. **36:**1203–1209.
3. **Black, J. G.** 1996. Microbiology: principles and applications, 3rd ed. Prentice Hall, Upper Saddle River, NJ.
4. **Boman, H.** 2003. Antibacterial peptides: basic facts and emerging concepts. J. Int. Med. **254:**197–215.
5. **Bradford, M. M.** 1976. A rapid and sensitive method for the quantitation of microgram quantities of protein utilizing the principle of protein-dye binding. Anal. Biochem. **72:**248–254.
6. **Brogden, K.** 2005. Antimicrobial peptides: pore formers or metabolic inhibitors in bacteria? Nat. Rev. Microbiol. **3:**238–250.
7. **Cavanagh, J., W. J. Fairbrother, A. G. Palmer, and N. J. Skelton.** 1996. Protein NMR spectroscopy: principles and practice. Academic Press, San Diego, CA.
8. **Chen, Y., et al.** 2005. Rational design of α-helical antimicrobial peptides with enhanced activities and specificity/therapeutic index. J. Biol. Chem. **280:** 12316–12329.
9. **Dennison, S. R., J. Wallace, F. Harris, and D. A. Phoenix.** 2005. Amphiphilic α-helical antimicrobial peptides and their structure/function relationships. Protein Pept. Lett. **12:**31–39.
10. **Gibbons, S., M. Oluwatuyi, and G. W. Kaatz.** 2003. A novel inhibitor of multidrug efflux pumps in *Staphylococcus aureus*. J. Antimicrob. Chemother. **51:**13–17.
11. **Giuliani, A. et al.** 2008. Antimicrobial peptides: natural templates for synthetic membrane-active compounds. Cell. Mol. Life Sci. **65:**2450–2460.
12. **Greenfield, N. J.** 2006. Using circular dichroism spectra to estimate protein secondary structure. Nat. Protoc. **1:**2876–2890.
13. **Hancock, R. E. W., and D. S. Chapple.** 1999. Peptide antibiotics. Antimicrob. Agents Chemother. **43:**1317–1323.
14. **Handler, A. A., J. E. Lim, and R. Losick.** 2008. Peptide inhibitor of cytokinesis during sporulation in Bacillus subtilis. Mol. Microbiol. **68:**588–599.
15. **Huang, H. W.** 2006. Molecular mechanisms of antimicrobial peptides: the origin of cooperativity. Biochim. Biophys. Acta **1758:**1292–1302.
16. **Huang, H. W.** 2009. Free energies of molecular bound states in lipid bilayers: lethal concentrations of antimicrobial peptides. Biophys. J. **96:**3263–3272.
17. **Huttunen-Hennelly, H. E. K.** 2010. An investigation into the N- and C-capping effects of glycine in cavitand-based four-helix bundle proteins. Bioorg. Chem. **38:**98–107.
18. **Huttunen-Hennelly, H. E. K., and J. C. Sherman.** 2007. The design, synthesis, and characterization of the first cavitand-based de novo hetero-template-assembled synthetic proteins (hetero-TASPs). Org. Biomol. Chem. **5:**3637–3650.
19. **Hwang, P. M., and H. J. Vogel.** 1998. Structure-function relationships of antimicrobial peptides. Biochem. Cell Biol. **76:**235–246.
20. **Jenssen, H., P. Hamill, and R. E. W. Hancock.** 2006. Peptide antimicrobial agents. Clin. Microbiol. Rev. **3:**491–511.
21. **Lippa, A. M., and M. Goulian.** 2009. Feedback inhibition in the PhoQ/PhoP signaling system by a membrane peptide. PLoS Genet. **5:**1–9.
22. **Lupa-Sieprawska, M., et al.** 2004. Degradation of human antimicrobial LL-37 by *Staphylococcus aureus*-derived proteinases. Antimicrob. Agents Chemother. **48:**4673–4679.
23. **Marqusee, S., and R. L. Baldwin.** 1987. Helix stabilization by Glu-Lys+ salt bridges in short peptides of *de novo* design. Proc. Natl. Acad. Sci. U. S. A. **84:**8898–8902.
24. **Matsuzaki, K., O. Murase, N. Fujii, and K. Miyajima.** 1996. An antimicrobial peptide, magainin 2, induced rapid flip-flop of phospholipids coupled with pore formation and peptide translocation. Biochemistry **35:**11361–11368.
25. **Matsuzaki, K., K. Sugishita, N. Fujii, and K. Miyajima.** 1996. Molecular basis for membrane selectivity of an antimicrobial peptide, magainin 2. Biochemistry **34:**3423–3429.
26. **Matsuzaki, K., K. Sugishita, M. Harada, N. Fujii, and K. Miyajima.** 1997. Interactions of an antimicrobial peptide, magainin 2, with outer and inner membranes of Gram-negative bacteria. Biochim. Biophys. Acta **1327:**119–130.
27. **Neville, F., et al.** 2006. Lipid headgroup discrimination by antimicrobial peptide LL-37: insight into mechanism of action. Biophys. J. **90:**1275–1287.
28. **Pace, C. N., and J. M. Scholtz.** 1998. A helix propensity based on experimental studies of peptides and proteins. Biophys. J. **75:**422–427.
29. **Podorieszach, A. P., and H. E. K. Huttunen-Hennelly.** 2010. The effects of tryptophan and hydrophobicity on the structure and bioactivity of novel indolicidin derivatives with promising pharmaceutical potential. Org. Biomol. Chem. **8:**1679–1687.
30. **Powers, J., and R. E. W. Hancock.** 2003. The relationship between peptide structure and antibacterial activity. Peptides **24:**1681–1691.
31. **Radek, K., and R. Gallo.** 2007. Antimicrobial peptides: natural effectors of the innate immune system. Semin. Immunopathol. **29:**27–43.
32. **Ramamoorthy, A., D. Lee, T. Narasimhaswamy, and R. P. R. Nanga.** 2010. Cholesterol reduces pardaxin's dynamics—a barrel-stave mechanism of membrane disruption investigated by solid-state NMR. Biochim. Biophys. Acta **1798:**223–227.
33. **Ross Friedman, C., B. B. Ross, and G. Martens.** 2009. Antibodies raised against tobacco aquaporins of the PIP2 class label the viscin tissue of the explosive dwarf mistletoe fruit. Plant Biol. **12:**229–233.
34. **Saxena, S., and C. Gomber.** 2010. Surmounting antimicrobial resistance in the millennium superbug: *Staphylococcus aureus*. Cent. Eur. J. Med. **5:**12–29.
35. **Schibli, D. J., R. F. Epand, H. J. Vogel, and R. M. Epan.** 2002. Tryptophan-rich antimicrobial peptides: comparative properties and membrane interactions. Biochem. Cell Biol. **88:**667–677.
36. **Sengupta, D., H. Leontiadou, A. E. Mark, and S. Marrink.** 2008. Toroidal pores formed by antimicrobial peptides show significant disorder. Biochim. Biophys. Acta **1778:**2308–2317.
37. **Shai, Y.** 1999. Mechanism of the binding, insertion and destabilization of phospholipid bilayer membranes by alpha-helical antimicrobial and cell nonselective membrane-lytic peptides. Biochim. Biophys. Acta **1462:**55–70.
38. **Stumpe, S., R. Schmid, D. L. Stephens, G. Georgiou, and E. P. Bakker.** 1998. Identification of OmpT as the protease that hydrolyzes the antimicrobial peptide protamine before it enters growing cells in *Escherichia coli*. J. Bacteriol. **180:**4002–4006.
39. **Wuthrich, K.** 1986. NMR of proteins and nucleic acids. Wiley, New York, NY.
40. **Yan, L., and M. E. Adams.** 1998. Lycotoxins, antimicrobial peptides from venom of the wolf spider Lycosa carolinesis. J. Biol. Chem. **273:**2059–2066.
41. **Yeaman, M. R., and N. Y. Yount.** 2003. Mechanisms of antimicrobial peptide action and resistance. Pharmacol. Rev. **55:**27–55.
42. **Zelezetsky, I., and A. Tossi.** 2006. Alpha-helical antimicrobial peptides—using a sequence template to guide structure-activity relationship studies. Biochim. Biophys. Acta **1758:**1436–1449.
43. **Zhu, W. L., et al.** 2006. Improvement of bacterial cell selectivity of melittin by a single trp mutation with a peptoid residue. Protein Pept. Lett. **13:**719–725.